Synthesis and characterization of gold nanoparticles biosynthesised from *Aspalathus linearis* (Burm.f.) R.Dahlgren for progressive macular hypomelanosis

Analike Blom van Staden [1], Daniela Kovacs [2], Giorgia Cardinali [2], Mauro Picardo [2], Maribanyana Lebeko [3], Nonhlanhla C. Khumalo [3], Suprakas Sinha Ray [4], Namrita Lall [1,5,6] *

[1] *Department of Plant and Soil Sciences, University of Pretoria, Pretoria, South Africa*

[2] *Cutaneous Physiopathology and Metabolomic Centre, San Gallicano Dermatological Institute, Rome, Italy*

[3] *Hair and Skin Research Lab, Division of Dermatology, University of Cape Town, Old Main Building Groote Schuur Hospital, Cape Town, South Africa*

[4] *DST-CSIR National Centre for Nanostructured Materials, Council for Scientific and Industrial Research, Pretoria 0001, South Africa*

[5] *School of Natural Resources, University of Missouri, USA*

[6] *College of Pharmacy, JSS Academy of Higher Education and Research, Mysuru 570015, India*

* Corresponding author: Namrita Lall. *E-mail address:* namrita.lall@up.ac.za; +27828404783; +27124202524

ABSTRACT

Introduction

The study investigated a natural solution for the hypopigmentary disorder, progressive macular hypomelanosis (PMH). The aim was to determine whether gold nanoparticles synthesized from *Aspalathus linearis* (Burm.f.) R.Dahlgren could be effective for PMH.

Methods

Gold nanoparticles (ALAuNPs) were synthesised using the ethanolic extract of *A. linearis* (AL_{EtOH}) and tested, along with the extract for its regulatory effect of melanogenesis in

human melanocytes and its antibacterial activity against *Cutibacterium acnes* (ATCC 6919 strain). Melanosome transfer was determined in a co-culture of normal human melanocytes and keratinocytes and was quantified using flow cytometry.

Results

The $ALAuNP_{stab}$ (AuNPs stabilized with gum arabic) and $ALAuNP_{non\text{-}stab}$ (non-stabilized) exhibited significantly ($P<0.001$) higher antibacterial activity against *C. acnes* with 50% inhibition at a concentration of 66.05 ± 1.10 µg/mL and 68.12 ± 1.05 µg/mL, respectively, as compared to that of AL_{EtOH} (271.20 ± 2.32 µg/mL). The AL_{EtOH} exhibited 50% reduction in cell proliferation (IC_{50} value) in human melanocytes at 345.5 ± 2.47 µg/mL, while $ALAuNP_{stab}$ and $ALAuNP_{non\text{-}stab}$ exhibited an IC_{50} value of 67.51 ± 1.12 and 69.63 ± 1.07 µg/mL, respectively. The AL_{EtOH} and $ALAuNP_{stab}$ tested at a concentration of 62.5 µg/mL, exhibited a significant increase ($P < 0.001$) in the total number of melanin present in human melanocytes compared to the untreated (control) cells. The cells treated with AL_{EtOH} and $ALAuNP_{stab}$ led to a significant ($P< 0.001$) increase in the number of melanosomes transferred as compared to the untreated cells.

Conclusion

This study confirmed that *A. linearis* and its biosynthesised gold nanoparticles stimulated melanin synthesis.

Keywords: *Aspalathus linearis, Cutibacterium acnes,* Gold nanoparticles, Melanin transfer, Progressive macular hypomelanosis

1. INTRODUCTION

Progressive macular hypomelanosis (PMH) can be identified by the white spots predominantly present on the back and chest. It has been reported that PMH lesioned skin

contained the precursors for melanosome development, however, the melanosomes contained less melanin and were undersized, which resulted in a reduction of melanosome transfer (Westerhof et al., 2004). Furthermore, PMH has been associated with the bacteria, *Cutibacterium acnes* (Barnard et al., 2016).

Current treatments for hypo-pigmentation disorders include surgical based therapies, phototherapy (using ultraviolet A (UVA) light), and steroidal therapies, however, these treatments resulted in negative systemic reactions (Hengge et al., 2006; Rigopoulos et al., 2004). Psoralen, or 8-methoxy psoralen, is a well-known photosensitizing compound that is used together with UVA light and is known as PUVA therapy (Halder and Rodney, 2012). PUVA has shown to be moderately effective in widespread vitiligo and progressive macular hypomelanosis, however, it was found that the hypopigmentation returned once the treatment was discontinued, therefore, it was recommended that the PUVA therapy be prolonged (Parsad et al., 2006). The side effects of long-term treatment include phototoxic reactions and photosensitivity, occasional hepatotoxicity, accelerated skin aging, and long-term carcinogenic risk (Halder and Rodney, 2012). The effective and ideal treatment, therefore, has not yet been identified.

Aspalathus linearis (Burm.f.) R. Dahlgren, commonly known as Rooibos, is indigenous to the Western Cape in South Africa, or more specifically, the Fynbos Biome of the Cape Floristic Region (Dahlgren and Glassman, 1968). The wild-growing populations of *A. linearis* are mostly found in the mountainous areas of the Northern Cape province, and the Western Cape's Cederberg mountains. The species prefers well-drained, nutrient-poor, highly acidic (pH 3 to 5.3) sandstone-derived soils (Dahlgren, 1988; Muofhe and Dakora, 2000). It has been established that *A. linearis* is indigenous to the Western Cape area, but the true origin and its bioprospecting history remains mostly undocumented. It was later documented by Van Wyk (2008) that the Rooibos species were traditionally used by the Khoi-San

communities as a general health tea. Current uses of *A. linearsis*, as obtained from the interviewed Wupperthal communities, are managing of high blood pressure, treatment of stomach related ailments such as colic and irritable bowel syndrome, relaxation, stress relief, hypotension and hypertension, diarrhoea and chest illnesses, kidney ailments, immune booster, blood circulation, oral health and stimulating appetite (Van Wyk, 2008).

The communities also used Rooibos for treating skin ailments such as nappy rash, eczema, minor skin wounds, acne, other dermatitis or for its soothing effects on irritated, inflamed and dry skin (Joubert et al., 2014). *Aspalathus linearis* is a versatile plant with several bioactivities. Two of these bioactivities, its significant antioxidant activity and antibacterial activity towards *Cutibacterium acnes*, indicated its potential use for hypopigmented disorders (Bramati et al., 2003; Joubert et al., 2004; Marnewick et al., 2005; Snijman et al., 2003; Tiedtke and Marks, 2002; Von Gadow et al., 1997). It has been reported that an increase in reactive oxygen species (ROS) led to melanocyte apoptosis and ultimately, a loss in melanocyte function (Zhang et al., 2014). Furthermore, *Cutibacterium acnes* has been associated with the hypopigmentary disorder, progressive macular hypomelanosis. It has been reported that the bacteria secretes factors that could potentially inhibit melanogenesis through the inhibition of tyrosinase (Westerhof et al., 2004). Therefore, this study investigated how *A. linearis* stimulated melanogenesis based on the information that it exhibited good antibacterial activity and is known for its antioxidant activity. Furthermore, this study aimed to find a natural solution for the hypopigmentary disorder, progressive macular hypomelanosis (PMH), and to determine whether gold nanoparticles synthesized from *A. linearis* could even be more effective than the ethanolic extract of *A. linearis.* Nanoscience and nanotechnology play a momentous role in revolutionizing medical diagnosis and treatment. Nanoparticles have been reported to successfuly increase the delivery of various herbal drugs, which led to increased bioavailability (Kesarwani and

Gupta, 2013). Gold nanoparticles have been studied as potential in transdermal delivery and could potentially lead to a treatment for hypopigmented disorders (Sonavane et al., 2008)

2. MATERIALS AND METHODS

2.1 Reagents and Bacteria

Normal human melanocytes and keratinocytes were obtained from the San Gallicano Dermatological Institute in Rome and the Hair and Skin Research Lab, University of Cape Town. The medium 254, supplemented with human melanocyte growth supplement, and medium 154 CF, supplemented with human keratinocyte growth supplement, were obtained from Thermo Fisher Scientific. All consumables and reference standards (≥98.0%, HPLC) were obtained from Sigma Aldrich, South Africa. The *Cutibacterium acnes* ATCC 6919 strain KWIK-STIK was obtained from Microbiologics (USA).

2.2 Plant Material Extraction

Aspalathus linearis (Burm.f.) R.Dahlgren (Fabaceae) plant material was donated by Rooibos Ltd (Production sample number: 588), Rooibos Avenue, Clanwilliam, GPS co-ordinates S 32° 11.131' EO 18° 53.291'. A voucher herbarium specimen (122176) was prepared and deposited at the H.G.W.J. Schweickerdt Herbarium, University of Pretoria, South Africa. The coarsely ground, dried, unfermented leaves and twigs (13.85 kg) of *A. linearis* was extracted with 34 L of ethanol and left at 25 °C for 20 days, shaking and stirring the container every second day. The extract (AL_{EtOH}) was filtered with a Buchi funnel (No 3-filter paper) and freeze-dried to a fine powder. The percentage yield of the freeze-dried extract was 9.03 % of the dried plant material.

2.3 Gas Chromatography – Time of Flight Mass Spectrometry

The GC-TOFMS analysis of the ethanolic extract of *A. linearis* was conducted using the method and the instrumentation described by Gorst-Allmana and Naude (2016). Briefly, the ethanolic extract of *A. linearis* was dissolved in methanol (anhydrous, 99.8%) to a concentration of 1 mg/mL. The splitless injection was operated in the splitless mode for 30 s after the injection of the sample. The data acquisition rate and the mass acquisition range were 10 spectra per second and 40−550 Da, respectively (Gorst-Allmana and Naude, 2016).

2.4 Synthesis and Characterization of Gold Nanoparticles using the Ethanolic Extract of *A. linearis*

The gold nanoparticles were synthesized using the ethanolic extract of *A. linearis.* For the reduction of the gold salts, 1 mL of the stock solution (18 mg/mL) of the $AL_{EtOH,}$ prepared in ethanol, was added to 17 mL of dH_2O and heated to 45 ºC. Gum arabic (36 mg) was used as a stabilizer in the stabilized sample, while it was omitted in the non-stabilized sample (Katti et al., 2009a).

Various analytical instruments were used to characterize the synthesized ALAuNPs, including UV-Vis (BIO-TEK Power-Wave XS multi-well plate reader (Thermo Fisher Scientific)), Transmission electron microscopy (TEM; JEOL JEM-2100F), Fourier-transform infrared spectroscopy (FTIR; Perkin Elmer Spectrum 100), dynamic light scattering (DLS; HORIBA LB 550 – a Bragg-Brentano geometry with a continuous scanning rate of 0.02 º/s and a scan range of $2\theta = 10–70^{o}$ was used to collect the diffraction measurements), X-ray powder diffraction (XRD, PANalytical X'Pert PRO – fitted with a Cu-Kα source (λ = 1.54184 Å) and set up at 45 kV and 40 mA) analysis and thermo-gravimetric analysis (TGA; Q500, TA Instruments – the sample was placed on the sample holder and heated under nitrogen at a rate of 10 ºC / min from 45 ºC to 900 ºC) (Elbagory et al., 2016).

2.5 Quantification of Pure Compounds using Ultra-Performance Liquid Chromatography – Quantitative Time of Flight. Twelve compounds previously isolated from *A. linearis* were quantified in AL_{EtOH} and ALAuNPs samples using a Waters Synapt G2 QTOF system and following the method described by Wooding et al. (2017). The compounds present in AL_{EtOH} and ALAuNPs samples were quantified by plotting a standard curve of each pure compound at five concentrations (250 µg/mL, 25 µg/mL, 2.5 µg/mL, 0.25 µg/mL, 0.025 µg/mL)(Wooding et al., 2017).

2.6 Analysing the Effect of the Ethanolic Extract of *A. linearis* and its Biosynthesised Gold Nanoparticles on *C. acnes* growth

The concentration to inhibit 50 % of bacterial growth (IC_{50}) was determined using a broth dilution method for the AL_{EtOH} and ALAuNPs samples against *C. acnes* ATCC 6919 strain (Mapunya et al., 2011). The method as described by van Staden et al. (2017) were followed in detail. Briefly, stock solutions of the AL_{EtOH} (2 mg/mL), ALAuNPs (2 mg/mL), and the positive control (tetracycline, 0.2 mg/mL) were prepared and serially diluted in 100 mL broth, to which 100 mL of the bacterial suspension was added. The solvent control was prepared by adding 2.5 % DMSO and 7.5 % dH_2O to the first wells and serially diluting (van Staden et al., 2017). Presto Blue, a cell viability indicator, was added to the plates after incubation for 72 hours in an anaerobic environment at 37 °C (De Canha et al., 2013). The fluorescence of the treatments was analyzed at 560 nm excitation and 590 nm emission using a VICTOR Nivo Elisa plate reader (Perkin Elmer).

2.7 *In vitro* Antiproliferation Assay with the Biosynthesised Gold Nanoparticles

The antiproliferation for AL_{EtOH}, $ALAuNP_{stab}$ and $ALAuNP_{non\text{-}stab}$ were determined on normal human melanocytes (NHM), cultured in medium 254 and supplemented with human

melanocyte growth supplement, $NaHCO_3$ (1.5 g/L), L-glutamate (2mM) and antibiotics (10 µg/mL streptomycin and 0.25 µg/mL fungizone). NHM were plated in 96 well plates (10 000 cells per well) and incubated overnight at 37 °C in 5 % CO_2.

Following incubation, the cells were treated for 24 hours with AL_{EtOH}, $ALAuNP_{stab}$, $ALAuNP_{non\text{-}stab,}$ and positive control (actinomycin D at 37 °C in 5 % CO_2). The final concentrations for the treatments, the positive control, and DMSO ranged from 400 to 3.13 µg/mL, 0.5 to 3.91 x 10^{-3} µg/mL, and 0.63 to 0.01 %, respectively. Proliferation was detected using the Presto blue reagent and quantified by measuring the fluorescence at 560 nm excitation and 590 nm emission using the Perkin Elmer VICTOR Nivo reader (Lall et al., 2007).

2.8 Determining the Effect of the Biosynthesised, using the Ethanolic Extract of *A. linearis,* Gold Nanoparticles *In Vitro* on Melanin Production

The stimulation of melanin production and melanin transfer was conducted to determine whether AL_{EtOH} and ALAuNPs could induce melanosome maturity in melanocytes. The method as described by van Staden et al. (2017) were followed in detail but was conducted on NHM instead of B16-F10 melanoma cells. The final concentrations for the treatments AL_{EtOH}, $ALAuNP_{stab,}$ and $ALAuNP_{non\text{-}stab}$ ranged between 7.8 and 250 µg/mL and 0.44 and 15 µg/mL for α-MSH, the positive control. The cells treated with 0.6 % DMSO and media were used as the negative and untreated control, respectively. Following incubation, the extracellular and intracellular melanin were separated and evaluated at 475 nm using the Perkin Elmer VICTOR Nivo reader (van Staden et al., 2017). The absorbance units obtained for the intracellular and extracellular melanosomes were used to determine the melanin concentration for the different treatments using a melanin standard curve as described by van Staden et al. (2017).

2.9 Melanosome Transfer

NHM cells (2500 cells/ well) and NHK cells (25 000 cells/ well) were seeded, at a 1:1 ratio of melanocyte and keratinocyte media, on gelatine treated round coverslips (13 mm diameter) and were incubated for 24 hours at 37 °C. The co-culture was treated with 62.5 µg/mL of AL_{EtOH} and $ALAuNP_{stab,}$ and 3.5 µg/mL of the positive control (αMSH) and again incubated for 24 hours. The percentage of DMSO present in the cells was 0.5 %. The treated cells were analyzed with immunofluorescence and compared to the untreated cells (Cardinali et al., 2008). The same procedure was followed for flow cytometry except the cells were not plated on round coverslips but directly in the plates.

2.10 Immunofluorescence

Melanin transfer in a co-culture treated with the ethanolic extract of *A. linearis* and its biosynthesised AuNP was observed using immunofluorescence. The method of Cardinali et al. (2008) was followed. Briefly, the co-cultured cells were stained with the primary antibodies, anti-mouse NKI/betab (1:100, ab34165, Abcam, Biocom Africa) and cytokeratin (1:200, ab9377, Abcam, Biocom Africa) for 1 hour at 25 °C. The washed cells were incubated for 1 hour at 25 °C with the secondary antibody mixture (Alexa 488 and Alexa 555, Invitrogen) at a ratio of 1:500 in PBS. The nuclei were stained with DAPI (4',6-diamidino-2-phenylindole, Invitrogen) prepared at a ratio of 1:1000 in PBS. The microscope slides were mounted using fluoroshield mounting media at 4 °C, and analyzed with a Zeiss Axioskop fluorescent microscope at a 20x magnification (Cardinali et al., 2008).

2.11 Flow Cytometry

The melanin transfer in a co-culture of melanocytes and keratinocytes, treated with the ethanolic extract of *A. linearis* and its biosynthesised AuNP, was quantified using flow cytometry. The treated cells were washed according to the BD Accuri C6 Plus manual and incubated with the primary antibodies anti-mouse NKI/betab (1:100, ab34165, Abcam, Biocom Africa) and cytokeratin (1:200, ab9377, Abcam, Biocom Africa) for 30 min at 25 °C. The washed cells were then incubated with the secondary antibodies conjugated to Alexa Fluor 488 (1:500, Invitrogen) and CruzFluor 594 (1:500, Santa Cruz Bio) for 30 min at 25 °C. Following incubation, the pellets were washed and re-suspended in FACS staining buffer containing 1x PBS, 1 % FCS and 0.01 % sodium azide. The treatments were analyzed with a BD Accuri C6 Plus flow cytometer preconfigured with green (533/30) and Orange (585/40) standard optical filters and using the FL1-A and FL2-A sensors.

2.12 Statistical Analysis

The experiments were repeated at least 3 times and performed in triplicates ($N = 3$) to ensure reproducible results. The 50 % inhibitory concentration values were determined using a 4-parameter logistic equation (Graph Pad Prism 5). Statistical significance was determined using a one-way analysis of variance together with Tukey's multiple comparison test in Graph Pad Prism 5.

3. RESULTS AND DISCUSSION

3.1 Gas Chromatography – Time of Flight Mass Spectrometry

Nineteen volatile compounds were identified in the ethanolic extract of *A. linearis* (AL_{EtOH}), of which oleamide was the predominant compound followed by 4-hydroxy-3-methyl-2-butenyl-acetate and benzothiazole (Table 1). Benzothiazole has been investigated for its numerous biological activities, including antitumor, antimalarial, and antibacterial activity

(Bradshaw and Westwell, 2004; Burger and Sawhney, 1968; Chohan et al., 2003). Oleamide has been reported for its anti-inflammatory activity, its use for Alzheimer's and in sleep therapy, and inhibits lipase which makes it useful in anti-acne products (González-Domínguez et al., 2014; Guan et al., 1997; Oh et al., 2010; Thompson, 1977). It has been reported that oleamide acts as a capping reagent of AuNPs (Anand et al., 2020). Therefore, AL_{EtOH}, was investigated for it reducing effect of AuNPs.

3.2 Synthesis and Identification of ALAuNPs

The formation of gold nanoparticles was observed by the color change from green to wine red after 2 min of stirring the mixture at 45 ºC. The formation of ALAuNPs (AuNPs synthesized with *A. linearis*) was confirmed spectrophotometrically by a UV absorption peak at 535 nm and microscopically using TEM by the observation of primarily (89%) spherical crystal structures (Figure 1). The remaining 11% of gold nanoparticles consisted of triangular, diamond-like and hexagonal shapes. Chen et al. (2005) reported that the shapes of the AuNP can be modified by the addition of salt or by changing the temperature. The temperature determines the absorption abilities of the chemical species and, therefore, influences the shape and size of the AuNPs. The sizes observed using TEM ranged between 4.89 and 37.89 nm in diameter for the gold nanoparticles stabilised with gum arabic ($ALAuNP_{stab}$) and between 6.71 and 45.71 nm for the non-stabilised gold nanoparticles ($ALAuNP_{non\text{-}stab}$). The crystallinity of the ALAuNPs was further confirmed, using XRD analysis, by peaks observed at 37º (2θ), 45º (2θ), 64º (2θ) and 78º (2θ). Additively, the Braggs reflections at the 111, 200, 220, and 311 lattice planes were representative of the face-centered cubic (fcc) of Au (Figure 2) (Stoeva et al., 2003).

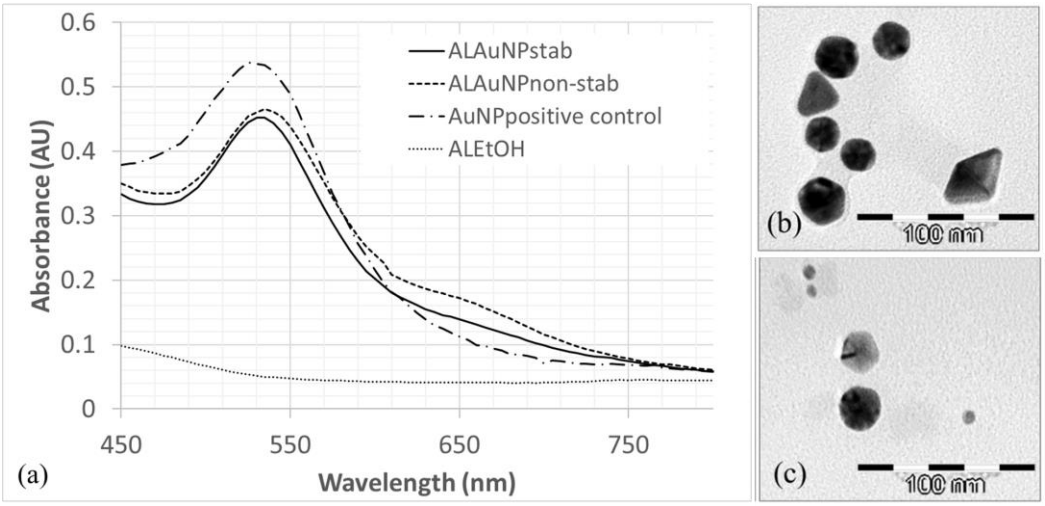

Figure 1. (a) UV–vis spectra of gold nanoparticles stabilized with gum arabic ($ALAuNP_{stab}$) and non-stabilized gold nanoparticles ($ALAuNP_{non\text{-}stab}$) synthesized from the ethanolic extract of *Aspalathus linearis* (AL_{EtOH}) and compared to the $AuNP_{positive\ control}$. The formation of gold nanoparticles was confirmed by a peak observed between 530 nm and 570 nm in the UV spectral scan. (b) TEM micrograph of $ALAuNP_{stab}$ at 100 nm, (c) TEM micrograph of $ALAuNP_{non\text{-}stab}$ at 100 nm.

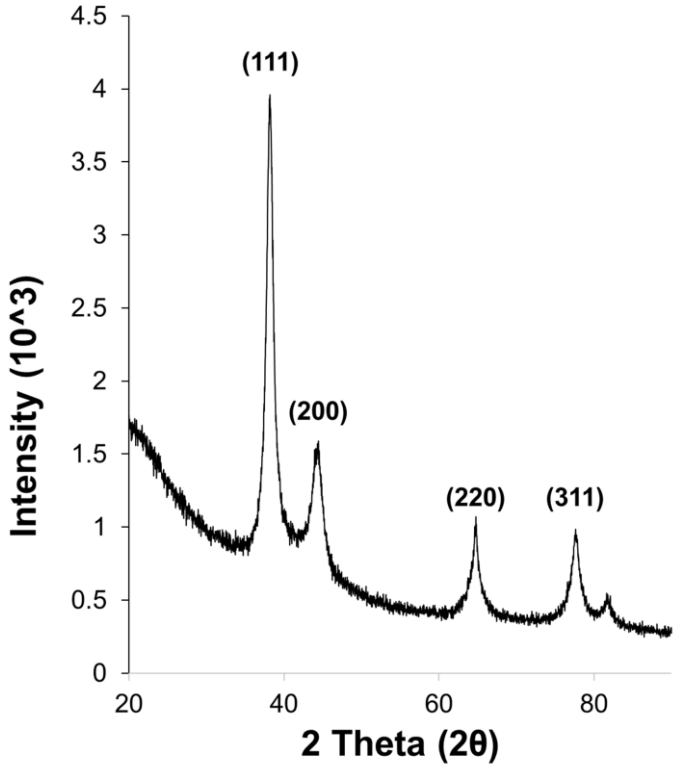

Figure 2. X-ray diffraction pattern of synthesized gold nanoparticles stabilized with gum arabic ($ALAuNP_{stab}$) and non-stabilized gold nanoparticles ($ALAuNP_{non\text{-}stab}$) displaying three major peaks corresponding to the 111, 200, 220 and 311 lattice planes representative of the face-centered cubic (fcc) of Au.

The average diameters of the $ALAuNP_{stab}$ and $ALAuNP_{non\text{-}stab}$, considering the plant's compounds coating the AuNPs, were determined using DLS analysis and were found to be 60.3 nm and 62.4 nm, respectively (Supplementary data Figure S1.). The dual coating of the gold nanoparticles by the gum arabic provided robust shielding and therefore prevented aggregation resulting in smaller $ALAuNP_{stab}$ when compared to the $ALAuNP_{non\text{-}stab}$ (Katti et al., 2009a). It was previously found that gum arabic together with a mixture of phytochemicals were responsible for the stabilization and synthesis of the AuNPs (Katti et al., 2009b). The thermal degradation properties of the organic shell around the ALAuNPs were determined using a TGA instrument over a temperature range of 90 ºC to 900 ºC. At 900 ºC, 22 % of the mass remained, representing the gold particles and indicating that the organic shell accounted for 78 % of the total weight content (Figure 3). It was determined that the phenolic content present in $ALAuNP_{stab}$, $ALAuNP_{non\text{-}stab}$ and $AuNP_{positive\ control}$ was 1319.62 µg/mL, 1020.59 µg/mL and 5497.8 µg/mL, respectively.

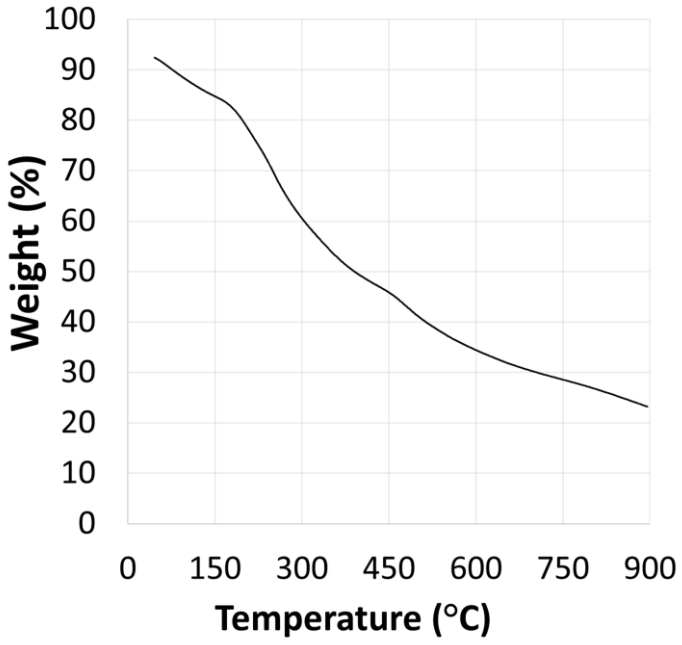

Figure 3. Thermal gravimetric analysis of gold nanoparticles synthesized with the ethanol extract of *Aspalathus linearis*. At 900 ºC, 22 % of the mass remained, representing the gold particles and indicating that the organic shell accounted for 78 % of the total weight content.

3.3 Stability of ALAuNPs

The stability of the ALAuNPs was determined by observing the plasmon (λ_{max}) in the different buffers, simulating biological environments, namely 0.5% bovine serum albumin (BSA), 0.5% cysteine, minimum essential medium (MEM) and 5% NaCl (Supplementary data Figure S2-S10.). The ALAuNPs showed minimal shifts in the plasmon and were, therefore, considered stable in all the buffers (pH 9 and pH 7) for seven days, especially at low (20 µg/mL and 40 µg/mL) concentrations. The stability of the ALAuNPs was similar to the results previously reported for AuNPs synthesized from fermented *A. linearis* (Elbagory et al., 2016).

3.4 Quantification of Pure Compounds Using Ultra-Performance Liquid Chromatography – Quantitative Time of Flight.

Twelve compounds previously identified in *A. linearis* were quantified in AL_{EtOH}, $ALAuNP_{stab,}$ and $ALAuNP_{non\text{-}stab}$ using Ultra-Performance Liquid Chromatography – Quantitative Time of Flight (Table 2). Aspalathin was found to be present in the highest quantities in AL_{EtOH}, $ALAuNP_{stab,}$ and $ALAuNP_{non\text{-}stab}$ at concentrations of 338.96 ± 1.90, 2.23 ± 0.06, 1.83 ± 0.03 $\mu g_{compound}/mg_{sample\ injected}$ respectivily. Orientin, one of the derivatives of aspalathin was found to be present in a good quantity at concentrations of 229.42 ± 0.45, 0.64 ± 0.024, 0.37 ± 0.01 $\mu g_{compound}/mg_{sample\ injected}$ for AL_{EtOH}, $ALAuNP_{stab,}$ and $ALAuNP_{non\text{-}stab}$, respectivily. The $ALAuNP_{stab}$ samples contained higher concentrations of caffeic acid, luteolin and rosmarinic acid than $AL_{EtOH,}$ indicating that those compounds had a higher percentage reducing potential of the gold nanoparticles compared to the other compounds.

3.5 FTIR Analysis of ALAuNPs

The AL_{EtOH}, $ALAuNP_{stab,}$ and $ALAuNP_{non\text{-}stab}$ were analyzed using FTIR, in the range of 600 to 4000 cm^{-1}, to determine the phytochemical groups responsible for reducing the gold salt to form AuNPs (Figure 4). The different functional groups detected on the ALAuNPs' surface were identified as follows: the band for ethers was located between 1000 and 1100 cm^{-1}, possibly representative of the cyclic ethers previously identified in *A. linearis*, namely aspalathin, (-)-epicatechin, isoquercitrin, luteolin, orientin, quercetin, vitexin, and the volatile compounds identified using GC-TOFMS analysis, namely 2,3-dihydro-5-methyl-furan and 2,5-dimethyl-2-(2-tetrahydrofuryl) tetrahydrofuran (Table 1) (Bramati et al., 2003).

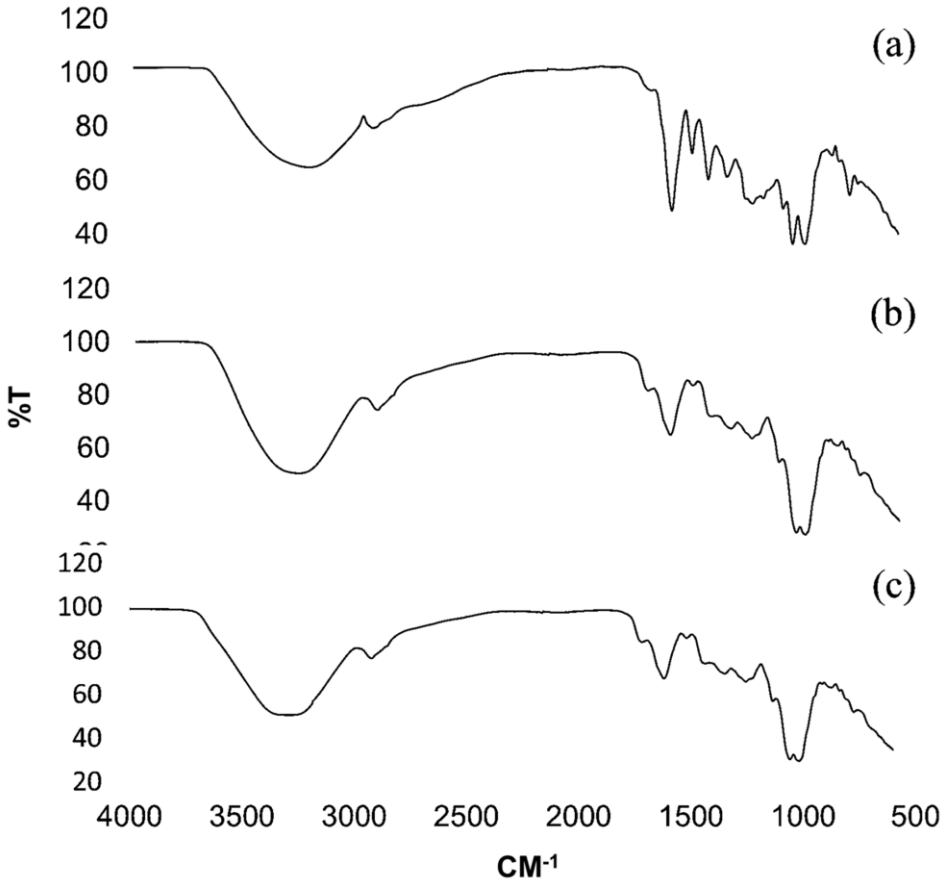

Figure 4. Fourier transform infrared spectra of (a) ethanol extract of *Aspalathus linearis* (AL_{EtOH}), (b) gold nanoparticles synthesized with $AL_{EtOH,}$ and stabilized with gum arabic (c) non-stabilized gold nanoparticles synthesized with $AL_{EtOH.}$

The small band at 1479 cm^{-1} is indicative of the presence of esters, which could be representative of any of the esters quantified in the AL_{EtOH}, such as 2-ethylhexyl trans-4-methoxycinnamate, 4-hydroxy-3-methyl-2-butenyl-acetate, dichloroacetic acid, 4-methylpentyl ester, 3-acetoxytridecane, ethyl undecanoate, and 2-propen-1-ol, 2-bromo-, acetate. The band for carboxylic acids, like those found in caffeic acid, 4-hydroxybenzoic acid, rosmarinic acid, and protocatechuic acid is typically situated at 3100 cm^{-1} (O-H) and 1720 cm^{-1} (C=O) (Iswaldi et al., 2011). Aromatic functional groups present in the majority of compounds are represented by the band situated around 700 cm^{-1}. The band for the amine group found in oleamide was situated at 3200 cm^{-1}. The FTIR results indicated that numerous phytochemicals groups act as reducing agents of gold salts (Katti et al., 2009b).

3.6 Antiproliferation

The AL_{EtOH} exhibited 50% cell viability reduction (IC_{50} value) on human melanocytes at 345.5 ± 2.47 µg/mL, which compared well with previously reported results which indicated that the IC_{50} value in normal skin cells was 260 µg/mL for the methanolic extract of *A. linearis* and 290 µg/mL for the aqueous extract of *A. linearis* (Magcwebeba et al., 2016). However, $ALAuNP_{stab}$ and $ALAuNP_{non\text{-}stab}$ exhibited an IC_{50} value of 67.51 ± 1.12 and 69.63 ± 1.07 µg/mL, respectively (Table 3). The antiproliferation could either be associated with the AuNPs as it has been reported that gold compounds exhibit varying degrees of antiproliferation towards a variety of cells, or it could be due to the partial coating of the AuNPs by caffeic acid, which has been reported for its cytotoxic effect (IC_{50} value of 15 µM) on B16F10 and melanoma cell lines (Kudugunti et al., 2011; Nune et al., 2009). Caffeic acid has been reported in low quantities in the *A. linearis*, and therefore, did not have an effect on the extract's antiproliferation, however, once caffeic acid-coated the AuNPs the available concentration could have been increased resulting in an increased antiproliferation (Krafczyk

and Glomb, 2008). There are no reports available for oleamide's antiproliferation against melanocytes.

3.7 Anti-bacterial Activity

The growth inhibitory potential of the ALAuNPs on *C. acnes* was significantly ($P<0.001$) higher than that of AL_{EtOH}. The ALAuNPs exhibited an IC_{50} value of 68.12 ± 1.05 and 66.05 ± 1.10 µg/mL for $ALAuNP_{non\text{-}stab}$ and $ALAuNP_{stab}$, respectively, while AL_{EtOH} only exhibited an IC_{50} value of 271.20 ± 2.32 µg/mL. Oleamide has been reported to inhibit lipases, the enzyme secreted by *C. acnes*, and thereby exhibited antibacterial activity (Oh et al., 2010). Therefore, the increased antibacterial activity of the AuNPs could be due to the oleamide coating the AuNPs. Alternatively, caffeic acid, which is potentially present in higher concentrations in the AuNPs due to the compound coating the nanoparticle, has been reported for its antibacterial activity towards gram-positive bacteria, which could potentially explain the significant ($P<0.001$) difference between the IC_{50} value of the ALAuNPs compared to that of the AL_{EtOH} (Table 1). Caffeic acid is a potent inhibitor of TNF-α (controls bacterial immunity and growth) and thereby could potentially inhibit the proliferation of *C. acnes* (Wang et al., 1992). Furthermore, the increased antibacterial activity observed for the ALAuNPs could be due to the increased penetration rate of AuNPs, with a diameter of 50 nm, than for larger molecules (Chithrani et al., 2006). The selectivity index for the samples were insignificant, therefore, it can be concluded that the antibacterial activity exhibited by the samples is due to the toxicity of the sample.

3.8 Melanin Production

The AL_{EtOH} and $ALAuNP_{stab}$ tested at a concentration of 62.5 µg/mL, exhibited a significant increase ($P < 0.001$) in the total number of melanin present after the 24-hour

treatment period compared to the untreated (control) cells (Figure 5), indicating that the samples stimulated melanin production in human melanocytes. There was no significant difference between AL_{EtOH} and $ALAuNP_{stab}$, however, using Beer's law (A (absorbance) = ε (molar absorptivity) x b (path length) x c (concentration of the compound in solution)), it was determined that the ALAuNPs consisted of 31.68 % of AL_{EtOH}. Therefore, to obtain the same bioactivity, 3 times less of AL_{EtOH} is required when using gold nanoparticles than when using the extract on its own. The results exhibited no significant difference between $ALAuNP_{non\text{-}stab}$ and the control for the total number of melanosomes, thereby indicating that $ALAuNP_{non\text{-}stab}$ did not stimulate melanin production. The reason for this could be the agglomeration of the AuNPs resulting in poor penetration of the melanocytes. Therefore, $ALAuNP_{non\text{-}stab}$ was excluded from further testing.

The cells treated with AL_{EtOH} and $ALAuNP_{stab}$ resulted in a higher number of extracellular melanosomes than intracellular melanosomes. However, the reduced number of intracellular melanosomes corresponded with the increase in the number of extracellular melanosomes present for the different samples. The results, therefore, indicated that the samples not only stimulated melanin production but also stimulated melanosome maturity and transfer. Melanin transfer induced by AL_{EtOH} and $ALAuNP_{stab}$ was confirmed using immunofluorescence and flow cytometry.

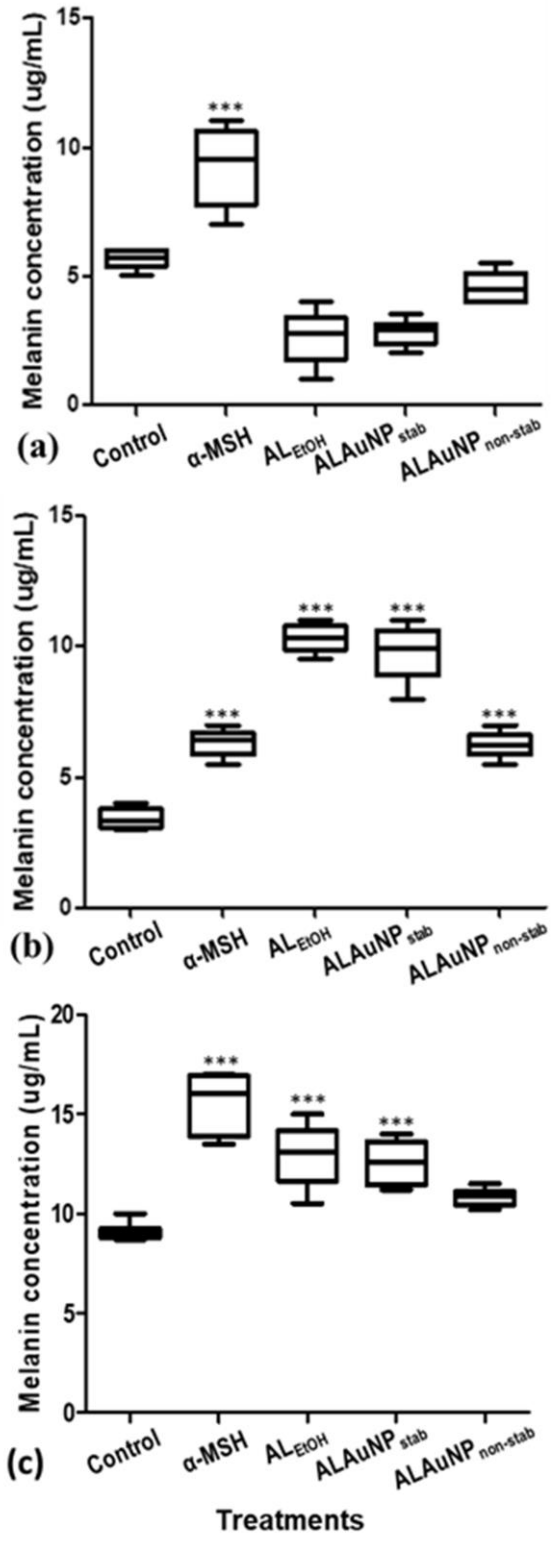

Figure 5. Graphs representing the concentration of melanin produced in human melanocytes treated with the positive control α-melanocyte stimulation hormone (α-MSH), the ethanol extract of *Aspalathus linearis* (AL_{EtOH}), the gold nanoparticles synthesized with AL_{EtOH} and stabilized with gum Arabic ($ALAuNP_{stab}$) and the non-stabilized gold nanoparticles synthesized with $AL_{EtOH.}$ ($ALAuNP_{non\text{-}stab}$), which were compared to the control (untreated cells). The effect of the treatments was determined on the (a) intracellular melanosomes, the (b) extracellular melanosomes, and the (c) total melanosomes.

3.9 Melanosome Transfer

The cells treated with AL_{EtOH}, $ALAuNP_{stab,}$ and α-MSH, showed an increase in the fluorescence at the dendrite's tips and a higher amount of peri-nuclear melanosome localization in the keratinocyte compared to that of the control (untreated) cells (Figure 6). Quantitative comparison was conducted of the positive (peri-nuclear melanosome localization) keratinocytes between the control cells, and the cells treated with α-MSH (10 μM), AL_{EtOH} (62.5 μg/mL) and $ALAuNP_{stab}$ (62.5 μg/mL) (Figure 7). The melanosome transfer stimulated by the treatments was found to be significantly ($P < 0.001$) higher compared to the control cells.

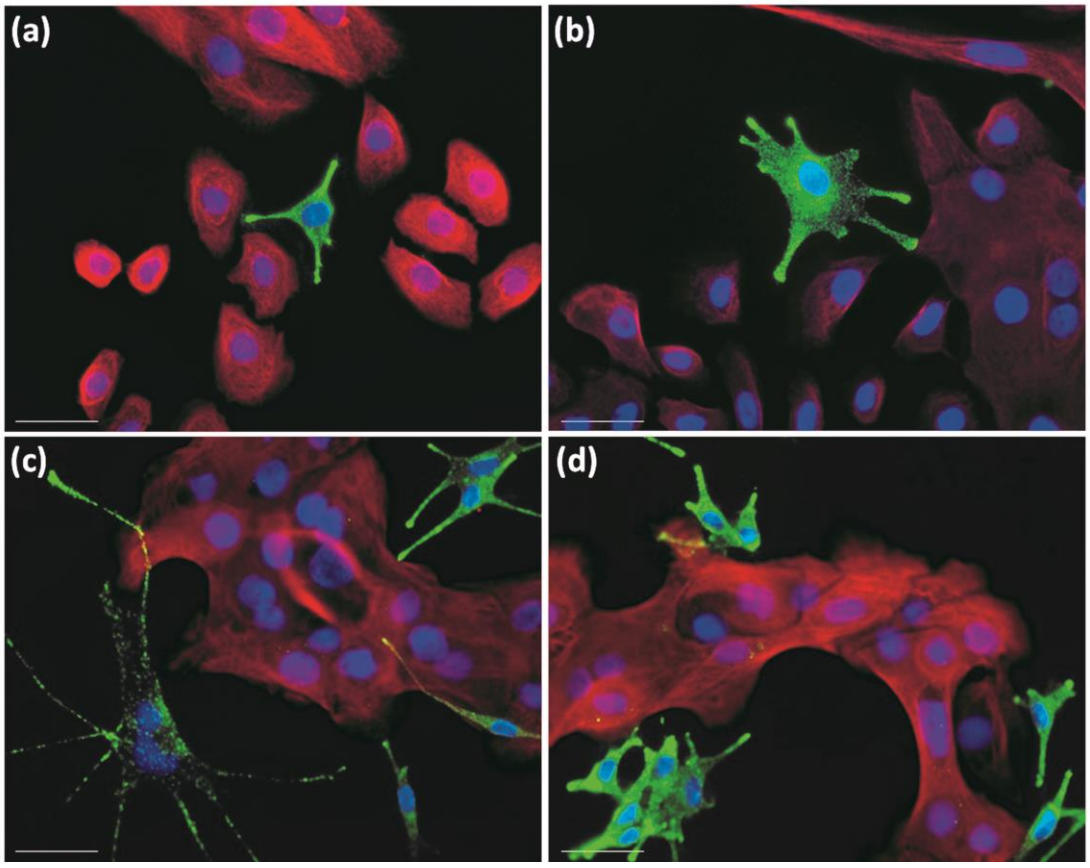

Figure 6. Immunofluorescent staining of a co-culture of human melanocytes and keratinocytes. The nuclei of the cells were stained blue (DAPI), the melanocytes stained green (NKI/betab) and keratinocytes stained red (Cytokeratin). The fluorescent microscope images indicated melanin transfer in (a) untreated (control) cells and cells treated with (b) α-MSH, (c) the ethanol extract of *Aspalathus linearis,* and (d) gum arabic stabilized gold nanoparticles. Green dots (melanosomes) present around the keratinocytes' nuclei indicated positive melanin transfer. The scale bar represents 10 μm.

The cells treated with AL_{EtOH} showed an increase in melanocyte dendricity and the concentration of melanosomes at the dendrite tips. It has been reported that phytoestrogens, known to be extracted with ethanol, upregulates cyclic adenosine monophosphate, which is linked to increased dendricity of the melanosomes, indicative of melanosome maturity and ultimately melanosome transfer (De Luca et al., 1993; Lee et al., 2005; Scott et al., 2006). Aspalathin, one of the main constituents of AL_{EtOH}, is a well-known phytoestrogen, therefore, aspalathin could possibly be responsible for the upregulation of melanin production and transfer (Clarke and Wiseman, 2008). Apart from phytoestrogens, it has been reported that quercetin is associated with increased dendrite protrusions (Takeyama et al., 2004). This is the first time that the effect of AL_{EtOH} and its synthesized gold nanoparticles on melanin production and transfer has been reported.

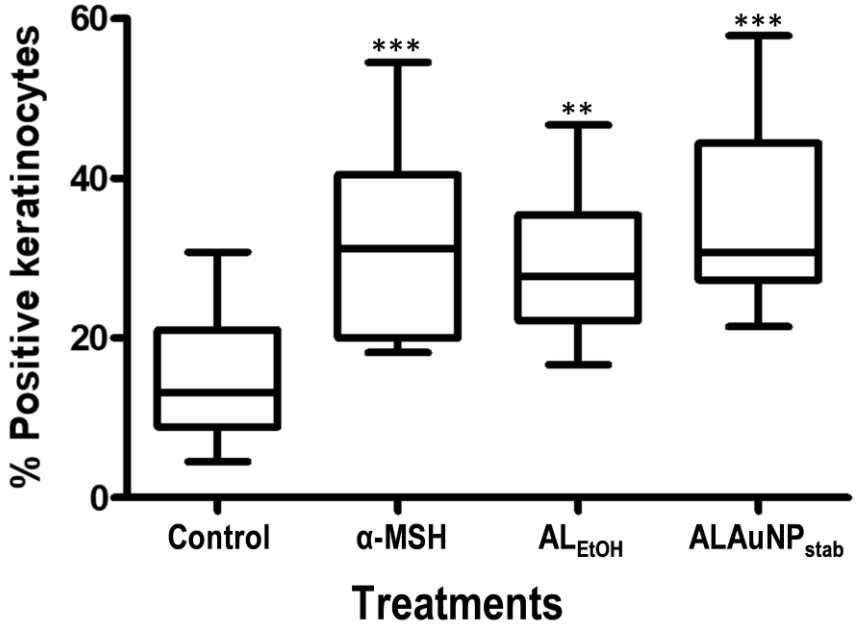

Figure 7. Quantitative comparison of the percentage positive keratinocytes (identified by melanosomes present around the nuclei, indicating melanin transfer), for the different treatments, namely, the untreated (control) cells, the positive control – α-melanocyte stimulating hormone (a-MSH) – at a concentration of 15 µg/ml, the ethanol extract of *Aspalathus linearis* (AL_{EtOH}) and the gold nanoparticles stabilized with gum arabic ($ALAuNP_{stab}$) at a concentration of 62.5 µg/ml.

The melanosome transfer observed with fluorescent microscopy was confirmed by flow cytometry. There was a significant ($P > 0.05$) increase in melanosome transfer in the treated cells compared to the untreated cells (Figure 8). An increase in melanosome transfer, indicated by the pixels in the upper right quadrant (Q4-UR) of the diagrams in Figure 8, of 3.9 % was observed for cells treated with the positive control (α-MSH), and 3.2% and 11.9% for AL_{EtOH} and $ALAuNP_{stab}$, respectively, compared to the untreated cells.

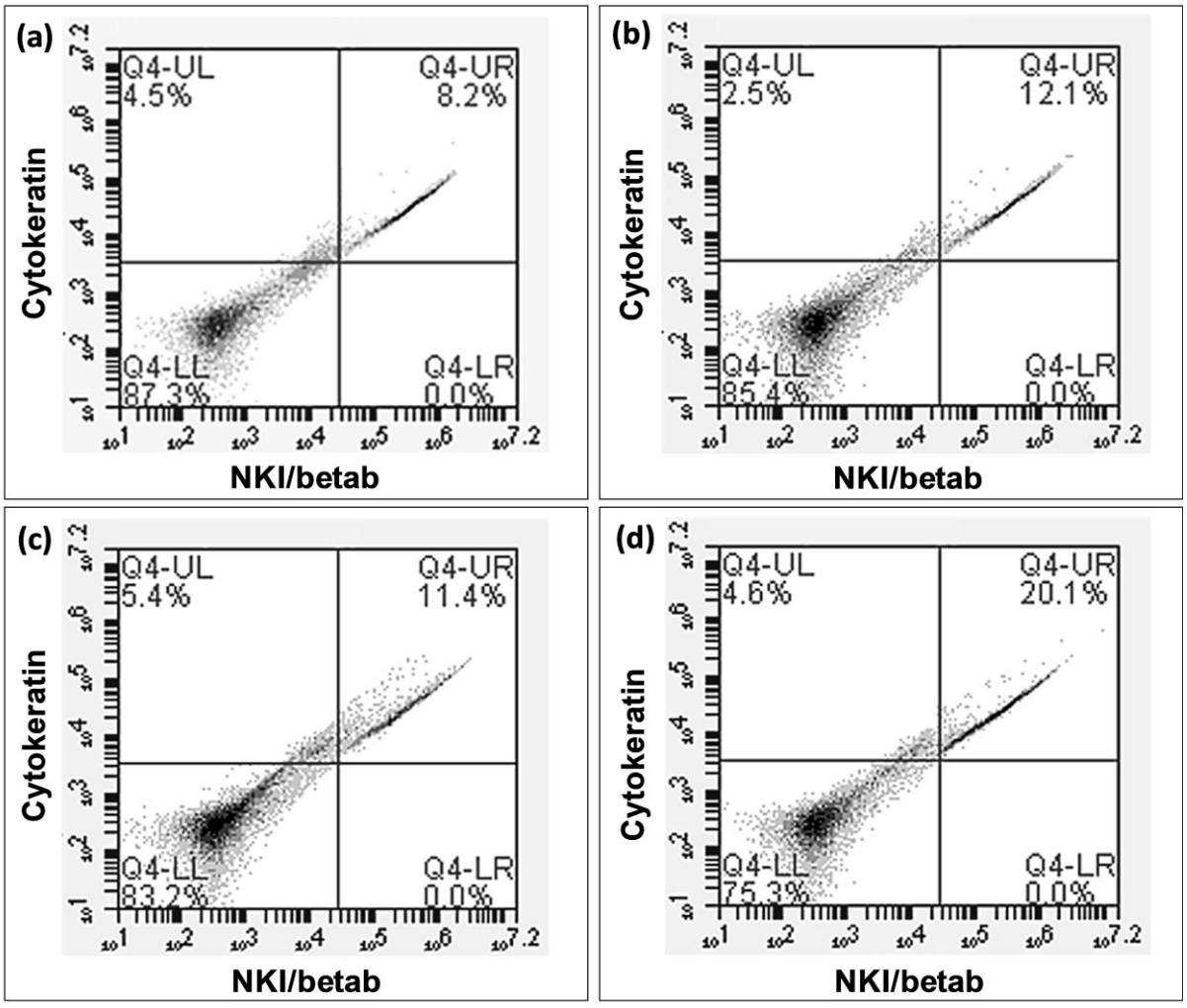

Figure 8. Flow cytometry of the (a) untreated cells and cells treated with (b) α-MSH (10 µM), (c) the ethanol extract of *Aspalathus linearis* (62.5 µg/mL) and (d) gum arabic stabilized gold nanoparticles (62.5 µg/mL). The treated cells stained with cytokeratin and NKI/betab was gated with unstained human melanocytes.

4. CONCLUSIONS

The present study for the first time reported the efficacy of the ethanolic extract of *A. linearis* (AL_{EtOH}) and its biosynthesised AuNPs against progressive macular hypomelanosis (PMH). Both AL_{EtOH} and its biosynthesised AuNPs exhibited antibacterial activity towards *C. acnes*, however, the biosynthesised AuNPs exhibited significantly ($P<0.001$) better antibacterial activity, when compared to AL_{EtOH}. Furthermore, AL_{EtOH} and its synthesized gold nanoparticles exhibited a significant ($P<0.001$) increase in melanogenesis at 62.5 µg/mL and could therefore potentially be used in a treatment for PMH. It was found that by using gold nanoparticles, 3 times less of AL_{EtOH} is required to elicit the same bioactivity. Future studies will focus on the permeation of the extract and clinical applications of the sample.

Conflict of Interests

The author declares that there is no conflict of interest regarding the publication of this paper.

Acknowledgments: The National Research Foundation for providing project funding. The University of Pretoria for providing the research facilities. Hair and Skin Research lab at the University of Cape Town (South Africa) and the San Gallicano dermatological institute (Italy) for sourcing and supplying the human melanocytes and keratinocytes. The DST-CSIR National Centre for Nanostructured Materials, Council for Scientific and Industrial Research, for the use of their nanoparticle characterization instruments.

Funding: This work was supported by the National Research Foundation, Innovation, and Scarce Skills Scholarships.

APPENDIX A. SUPPLEMENTARY DATA

The dynamic light scattering plot and the UV-Vis gold nanoparticles stability data graphs are available as Supplementary data.

References

Anand, K. et al., 2020. Human serum albumin interaction, in silico and anticancer evaluation of Pine-Gold nanoparticles. Process Biochem. 89, 98-109.

Barnard, E. et al., 2016. Strains of the *Propionibacterium acnes* type III lineage are associated with the skin condition progressive macular hypomelanosis. Sci. Rep. 31968, 1-9. https://doi.org/10.1038/srep31968

Bradshaw, T., Westwell, A., 2004. The development of the antitumour benzothiazole prodrug, Phortress, as a clinical candidate. Curr. Med. Chem. 11, 1009-1021. https://doi.org/10.2174/0929867043455530

Bramati, L., Aquilano, F., Pietta, P., 2003. Unfermented rooibos tea: quantitative characterization of flavonoids by HPLC−UV and determination of the total antioxidant activity. J. Agric. Food Chem. 51, 7472-7474. https://doi.org/10.1021/jf0347721

Burger, A., Sawhney, S., 1968. Antimalarials. III. Benzothiazole amino alcohols. J. Med. Chem. 11, 270-273. https://doi.org/10.1021/jm00308a018

Cardinali, G., Bolasco, G., Aspite, N., Lucania, G., Lotti, L.V., Torrisi, M.R., Picardo, M., 2008. Melanosome transfer promoted by keratinocyte growth factor in light and dark skin-derived keratinocytes. J. Investig. Dermatol. 128, 558-567. https://doi.org/10.1038/sj.jid.5701063

Chithrani, B.D., Ghazani, A.A., Chan, W.C., 2006. Determining the size and shape dependence of gold nanoparticle uptake into mammalian cells. Nano Lett. 6, 662-668. https://doi.org/10.1021/nl052396o

Chohan, Z.H., Scozzafava, A., Supuran, C.T., 2003. Zinc complexes of benzothiazole-derived Schiff bases with antibacterial activity. J. Enzyme Inhib. Med. Chem. 18, 259-263. https://doi.org/10.1080/1475636031000071817

Clarke, D., Wiseman, H., 2008. Phytoestrogens. Bioactive Compounds in Foods. Blackwell Publishing, Oxford

De Canha, M., Berrington, D., Lall, N., CJ, H.-S., Oosthuizen, C., 2013. Viability reagent, prestoblue, in comparison with other available reagents, utilized in cytotoxicity and antimicrobial assays. Int. J. Microbiol. 2013, 1-5. https://doi.org/10.1155/2013/420601

De Luca, M., Siegrist, W., Bondanza, S., Mathor, M., Cancedda, R., Eberle, A.N., 1993. Alpha melanocyte stimulating hormone (alpha MSH) stimulates normal human melanocyte growth by binding to high-affinity receptors. J. Cell Sci. 105, 1079-1084.

Elbagory, A.M., Cupido, C.N., Meyer, M., Hussein, A.A., 2016. Large scale screening of Southern African plant extracts for the green synthesis of gold nanoparticles using microtitre-plate method. Molecules. 21, 1498. https://doi.org/10.3390/molecules21111498

González-Domínguez, R., García-Barrera, T., Gómez-Ariza, J.L., 2014. Metabolomic study of lipids in serum for biomarker discovery in Alzheimer's disease using direct infusion mass spectrometry. J. Pharm. Biomed. Anal. 98, 321-326. https://doi.org/10.1016/j.jpba.2014.05.023

Gorst-Allmana, C.P., Naude, Y., 2016. Fynbos products: what's in the bottle? An investigation of terpenoid constituents in fynbos products by GCxGC-TOFMS and GC-HRT. S. Afr. J. Chem. 69, 213-217. https://doi.org/10.17159/0379-4350/2016/v69a27

Guan, X., Cravatt, B.F., Ehring, G.R., Hall, J.E., Boger, D.L., Lerner, R.A., Gilula, N.B., 1997. The sleep-inducing lipid oleamide deconvolutes gap junction communication and calcium wave transmission in glial cells. Int. J. Cell Biol. 139, 1785-1792. https://doi.org/10.1083/jcb.139.7.1785

Halder, R.M., Rodney, I.J., 2012. Disorders of Hypopigmentation. Skin of Color: a practical guide to dermatologic diagnosis and treatment. Springer, New York

Hengge, U.R., Ruzicka, T., Schwartz, R.A., Cork, M.J., 2006. Adverse effects of topical glucocorticosteroids. J. Am. Acad. Dermatol. 54, 1-15. https://doi.org/0.1016/j.jaad.2005.01.010

Iswaldi, I., Arráez-Román, D., Rodríguez-Medina, I., Beltrán-Debón, R., Joven, J., Segura-Carretero, A., Fernández-Gutiérrez, A., 2011. Identification of phenolic compounds in aqueous and ethanolic rooibos extracts (*Aspalathus linearis*) by HPLC-ESI-MS (TOF/IT). Anal. Bioanal. Chem. 400, 3643-3654. https://doi.org/10.1007/s00216-011-4998-z

Katti, K. et al., 2009. Green nanotechnology from cumin phytochemicals: generation of biocompatible gold nanoparticles. Int. J. Green Nanotechnol. Biomed. 1, B39-B52. https://doi.org/10.1080/19430850902931599

Kesarwani, K., Gupta, R., 2013. Bioavailability enhancers of herbal origin: An overview. Asian Pac. J. Trop. Biomed. 3, 253-266. https://doi.org/10.1016/S2221-1691(13)60060-X

Krafczyk, N., Glomb, M.A., 2008. Characterization of phenolic compounds in rooibos tea. J. Agric. Food Chem. 56, 3368-3376. https://doi.org/10.1021/jf703701n

Kudugunti, S.K., Vad, N.M., Ekogbo, E., Moridani, M.Y., 2011. Efficacy of caffeic acid phenethyl ester (CAPE) in skin B16-F0 melanoma tumor bearing C57BL/6 mice. Invest. New Drugs. 29, 52-62. https://doi.org/10.1007/s10637-009-9334-5

Lall, N., Mapunya, M., Nikolova, R., Houghton, P., 2007. Anti-tyrosinase activity of South African plant extracts. Planta Medica. 73, 464. https://doi.org/10.1055/s-2007-987244

Lee, J. et al., 2005. Glycyrrhizin induces melanogenesis by elevating a cAMP level in B16 melanoma cells. J. Invest. Dermatol. 124, 405-411. https://doi.org/10.1111/j.0022-202X.2004.23606.x

Magcwebeba, T.U. et al., 2016. The potential role of polyphenols in the modulation of skin cell viability by *Aspalathus linearis* and *Cyclopia* spp. herbal tea extracts in vitro. J. Pharm. Pharmacol. 68, 1440-1453. https://doi.org/10.1111/jphp.12629

Mapunya, M.B., Hussein, A.A., Rodriguez, B., Lall, N., 2011. Tyrosinase activity of *Greyia flanaganii* (Bolus) constituents. Phytomedicine. 18, 1006-1012. https://doi.org/10.1016/j.phymed.2011.03.013

Muofhe, M.L., Dakora, F.D., 2000. Modification of rhizosphere pH by the symbiotic legume *Aspalathus linearis* growing in a sandy acidic soil. Funct. Plant Biol. 27, 1169-1173.

Nune, S.K. et al., 2009. Green nanotechnology from tea: phytochemicals in tea as building blocks for production of biocompatible gold nanoparticles. J. Mater. Chem. 19, 2912-2920. https://doi.org/10.1039/b822015h

Oh, Y.T., Lee, J.Y., Lee, J., Lee, J.H., Kim, J.-E., Ha, J., Kang, I., 2010. Oleamide suppresses lipopolysaccharide-induced expression of iNOS and COX-2 through inhibition of NF-κB activation in BV2 murine microglial cells. Neurosci. Lett. 474, 148-153. https://doi.org/10.1016/j.neulet.2010.03.026

Parsad, D., Kanwar, A., Kumar, B., 2006. Psoralen–ultraviolet A vs. narrow-band ultraviolet B phototherapy for the treatment of vitiligo. J. Eur. Acad. Dermatol. Venereol. 20, 175-177. https://doi.org/10.1111/j.1468-3083.2006.01413.x

Rigopoulos, D., Ioannides, D., Kalogeromitros, D., Gregoriou, S., Katsambas, A., 2004. Pimecrolimus cream 1% vs. betamethasone 17-valerate 0· 1% cream in the treatment

of seborrhoeic dermatitis. A randomized open-label clinical trial. Br. J. Dermatol. 151, 1071-1075. https://doi.org/10.1111/j.1365-2133.2004.06208.x

Scott, G.A., Jacobs, S.E., Pentland, A.P., 2006. sPLA2-X stimulates cutaneous melanocyte dendricity and pigmentation through a lysophosphatidylcholine-dependent mechanism. J. Invest. Dermatol. 126, 855-861. https://doi.org/10.1038/sj.jid.5700180

Sonavane, G., Tomoda, K., Sano, A., Ohshima, H., Terada, H., Makino, K., 2008. In vitro permeation of gold nanoparticles through rat skin and rat intestine: effect of particle size. Colloids Surf B. 65, 1-10. https://doi.org/10.1016/j.colsurfb.2008.02.013

Stoeva, S.I., Prasad, B., Uma, S., Stoimenov, P.K., Zaikovski, V., Sorensen, C.M., Klabunde, K.J., 2003. Face-centered cubic and hexagonal closed-packed nanocrystal superlattices of gold nanoparticles prepared by different methods. J. Phys. Chem. B. 107, 7441-7448. https://doi.org/10.1021/jp030013+

Takeyama, R., Takekoshi, S., Nagata, H., Osamura, R.Y., Kawana, S., 2004. Quercetin-induced melanogenesis in a reconstituted three-dimensional human epidermal model. J. Mol. Histol. 35, 157-165. https://doi.org/10.1023/B:HIJO.0000023388.51625.6c

Thompson, G.F., 1977. Medicament preparations. Google Patents,

van Staden, A.B., De Canha, M., Nqephe, M., Rademan, S., Kumar, V., Lall, N., 2017. Potential medicinal plants for progressive macular hypomelanosis. S. Afr. J. Bot. 111, 346-357. https://doi.org/10.1016/j.sajb.2017.04.007

Van Wyk, B.-E., 2008. A broad review of commercially important southern African medicinal plants. J. Ethnopharmacol.. 119, 342-355. https://doi.org/10.1016/j.jep.2008.05.029

Wang, L.J., Brännström, M., Robertson, S.A., Norman, R.J., 1992. Tumor necrosis factor α in the human ovary: presence in follicular fluid and effects on cell proliferation and

prostaglandin production. Fertil. Steril. 58, 934-940. https://doi.org/10.1016/S0015-0282(16)55438-7

Westerhof, W., Relyveld, G.N., Kingswijk, M.M., de Man, P., Menke, H.E., 2004. *Propionibacterium acnes* and the pathogenesis of progressive macular hypomelanosis. Arch. Dermatol.. 140, 210-214. https://doi.org/10.1001/archderm.140.2.210

Wooding, M., Bradfield, J., Maharaj, V., Koot, D., Wadley, L., Prinsloo, L., Lombard, M., 2017. Potential for identifying plant-based toxins on San hunter-gatherer arrowheads. S. Afr. J. Sci. 113, 1-10. http://dx.doi.org/10.17159/sajs.2017/20160210

Table 1 Chemical compounds present in the ethanolic extract of unfermented *Aspalathus linearis* quantified using Gas Chromatography – Time of Flight Mass Spectrometry

Chemical compounds	% of volatile compounds in *A. linearis*
2,3-dihydro-5-methyl-furan	9.50
Benzothiazole	10.05
5-Nonen-2-one	2.61
2,7-Octanedione	8.99
4-hydroxy-3-methyl-2-butenyl-acetate	10.73
2,5-Dimethyl-2-(2-tetrahydrofuryl) tetrahydrofuran	3.19
6-bromo-2-Hexanone	3.09
2-Propen-1-ol, 2-bromo-, acetate	0.65
1-C-methyl-scyllo-Inositol	2.77
Dichloroacetic acid, 4-methylpentyl ester	4.64
Ethyl undecanoate	0.44
Menthol, 1'-(butyn-3-one-1-yl)-, (1S,2S,5R)-	1.58
Trans-farnesol	2.18
Octahydrobenzo[b]pyran, 4a-acetoxy-5,5,8a-trimethyl-	0.70
3-Acetoxytridecane	3.98
3-(5-Methyl-furyl)-N-furamidopropionamide	0.91
(Z)-9-Octadecenamide (Oleamide)	31.70
2-Ethylhexyl trans-4-methoxycinnamate	0.47
Hexanedioic acid, bis(2-ethylhexyl) ester	1.82

Table 2 Chemical compounds present in the ethanolic extract of unfermented *Aspalathus linearis* and its biosynthesised gold nanoparticles quantified using Ultra-Performance Liquid Chromatography – Quantitative Time of Flight

Compounds	Quantification ($\mu g_{compound}/mg_{sample\ injected} \pm SD^c$)			Mode	Calibration curve	R^2	LOD[e] (ppm)	LOQ[f] (ppm)
	AL_{EtOH}	$ALAuNP_{stab}$[a]	$ALAuNP_{non\text{-}stab}$[b]					
Aspalathin	338.96 ± 1.90	2.23 ± 0.06	1.83 ± 0.03	Positive	y = 26.882x	0.999	< 0.25	< 2.5
Caffeic acid	0.05 ± 0.003	0.10 ± 0.007	0.001 ± 0.001	Negative	y = 9.7504x	0.999	< 0.25	< 2.5
(-)-Epicatechin	5.71 ± 0.08	0.008 ± 0.0003	0.009 ± 0.003	Negative	y = 14.015x	0.999	< 0.25	< 0.25
4-Hydroxybenzoic acid	3.07 ± 0.41	2.03 ± 0.04	0.77 ± 0.015	Negative	y = 2.3093x	0.999	< 25	< 25
Isoquercitrin	5.07 ± 1.10	0.49 ± 0.0007	0.29 ± 0.0004	Negative	y = 15.087x	0.999	< 25	< 25
Luteolin	0.01 ± 0.02	0.46 ± 0.004	0.008 ± 0.0008	Positive	y = 54.481x	0.999	< 0.25	< 2.5
Orientin	229.42 ± 0.45	0.64 ± 0.024	0.37 ± 0.01	Positive	y = 54.864x	0.981	< 0.25	< 2.5
n-Propyl gallate	0.46 ± 0.02	0.44 ± 0.0005	0.40 ± 0.0004	Negative	y = 77.076x	0.992	< 0.25	< 0.25
Protocatechuic acid	1.31 ± 0.55	0.22 ± 0.0001	0.14 ± 0.0001	Negative	y = 33.755x	0.999	< 2.5	< 2.5
Quercetin	8.61 ± 0.43	0.03 ± 0.0008	0.004 ± 0.0001	Positive	y = 37.227x	0.995	< 2.5	< 2.5
Rosmarinic acid	0.24 ± 0.09	0.44 ± 0.0002	0.15 ± 0.0001	Negative	y = 33.755x	0.995	< 25	< 25
Vitexin	5.61 ± 0.59	0.28 ± 0.015	0.13 ± 0.004	Positive	y = 159.86x	0.996	< 0.025	< 0.25

[a]AuNPs stabilized with gum arabic, [b]non-stabilised AuNPs, [c]Standard deviation, [e]Limit of Detection, [f]Limit of quantification.

Table 3 The fifty percent cell proliferation inhibitory concentration (IC_{50}) against human melanocytes and 50% inhibitory concentration against *Cutibacterium acnes* (AtCC 6919) of the EtOH extract of *Aspalathus linearis* (AL_{EtOH}) and the gold nanoparticles synthesized with AL_{EtOH}.

Treatment	Antiproliferation assay IC_{50} (µg/mL) ± SD[e]	Antibacterial assay IC_{50} (µg/mL) ± SD[e]	Selectivity Index[f]
AL_{EtOH}	345.50 ± 2.47	271.20 ± 2.32	1.27
$ALAuNP_{stab}$[a]	67.51 ± 1.12	66.05 ± 1.10	1.02
$ALAuNP_{non\text{-}stab}$[b]	69.63 ± 1.07	68.12 ± 1.05	1.02
$AuNP_{positive\ control}$	>400	>500	N/A
Actinomycin D[c]	0.039 ± 0.002	-	N/A
Kojic acid[d]	-	1.86 ± 0.24	N/A

[a]AuNPs stabilised with gum arabic, [b]non-stabilised AuNPs [c]positive controls for the antiproliferation assay, [d] positive controls for the antibacterial assay; [e]Standard deviation; [f]The selectivity index was calculated by dividing the IC_{50} value in the antiproliferation assay by the IC_{50} value in the antibacterial assay. A high selectivity is when SI ≥ 3.